Pressure Effect on Solvation Dynamics in Micellar Environment

Kimihiko Hara,* Hiroaki Kuwabara, and Okitsugu Kajimoto

Division of Chemistry, Graduate School of Science, Kyoto University, Sakyo-ku, Kyoto 606-8502, Japan

Received: March 15, 2001; In Final Form: May 22, 2001

Solvation dynamics of an excited solvatochromic probe molecule in micellar environment has been studied as a function of pressure. In addition to steady-state spectrum, time-dependent fluorescence Stokes shift of coumarin 153 in aqueous solution of typical neutral surfactant Triton X-100 was measured at high pressures using time-correlated single-photon counting techniques with a time-resolution of 20 ps. It was found that polarity of the microenvironment decreases with increasing pressure. The solvation dynamics exhibits bimodal relaxation behavior with two characteristic time constants of 198 ps and 1.63 ns at atmospheric pressure. The solvation time becomes shorter with increasing pressure. The bimodal relaxation and its pressure dependence is considered as closely connected with the pressure effect on the hydrogen bonding of water molecules. And also the model assuming an equilibrium between "bound water" and "free water" within the Stern layer of micelles is discussed.

1. Introduction

Over the past few decades, numerical experimental and theoretical studies have been devoted to polar solvation dynamics in homogeneous pure solutions. Especially the studies of polar solvation dynamics by means of fluorescence probe method using coumarin derivatives as solute probes have been widely performed.[1]

The structure and the behavior of solvation dynamics of restricted water molecules in the hydration shell of molecular aggregated systems or biomolecules have been the subject of recent studies.[2−14] The structure and solvation dynamics of water molecules in these environments are considered as quite different from those of pure bulk liquid.

For a complete knowledge of the function of molecular aggregated systems such as micelles, proteins, inclusion compounds, and lipid membranes, an understanding the dynamics of the aqueous environment surrounding them is essential, since the water molecules located in such confined or restricted environments are expected to play an important role in various natural and biological aggregated systems. Recently the dynamic properties of water molecules in the vicinity of such aggregated systems have been extensively studied by Bhattacharyya et al.,[6−8,10−14] reporting the relaxation time appreciably different scale from that in bulk water. Namely, pure water molecules exhibit the solvation dynamics with subpicosecond time scale,[2] whereas the solvation dynamics of aggregated systems, such as cyclodextrin and micelles, are likely to be reduced by several orders of magnitude.[2−14] This has been explained by freezing of the translational modes of water molecule within the restricted cavity.[15] In Table 1, the solvation times reported for various molecular aggregated systems are compared. Note that, in every system, the solvation dynamics is bimodal. Those time data, however, are too dispersive and chaotic to deduce any systematic conclusion.

One useful approach to this problem is to change the pressure, where the pressure effect on the solvation structure is preferably small, yet the dynamical properties are markedly changed with a single probe molecule[16,17] Pressure causes the time scale of diffusive dynamics to be slower, so that the fast dynamics at atmospheric pressure may be shifted to slower and enables us to observe at high pressures with a longer well-detectable time scale. Furthermore, the high-pressure study may be useful for discriminating the diffusive process from nondiffusive (or inertial) relaxation process.

In this paper we report the results of pressure effect on the solvation dynamics of water molecules around a probe solute in micellar environment. Here we adopted as a model for the restricted space system, coumarin 153 (C153) solubilized in the typical neutral micelles of Triton X-100 (TX-100).[18] Their molecular structures are shown in Figure 1. The pressure

TABLE 1: Solvation Times of Micelles and Various other Molecular Aggregated Systems

	probe	τ_1 (a_1) (ps)	τ_2 (a_2) (ps)	ref
(i) micelle				
TX-100[a]	C480[b]	550 (0.51)	2400 (0.49)	6
	DCM[d]	300 (0.15)	2440 (0.85)	12
	4AP[c]	330 (0.59)	1270 (0.41)	11
SDS[e]	C480	180 (0.74)	2140 (0.26)	6
	DCM	160 (0.55)	2900 (0.45)	12
	4AP	82 (1.0)		11
CTAB[f]	C480	285 (0.4)	630 (0.6)	6
	DCM	170 (0.5)	630 (0.5)	12
	4AP	100 (0.39)	383 (0.61)	11
(ii) inclusion compound				
γCD[g]	C480	109 (0.36)	1200 (0.36)	2
(iii) water pool of reverse micelle				
AOT[h]	C480	1700 (0.5)	12000 (0.5)	7
	4AP	340 (0.67)	5000 (0.33)	8
(iv) vesicle				
DMPC[i]	C480	600 (0.4)	11000 (0.6)	10
	DCM	230 (0.4)	1600 (0.6)	13

[a] Triton X-100. [b] Coumarin, 480. [c] 4-Aminophthalimide. [d] 4-(Dicyanomethylene)-2-methyl-6(p-dimethylaminostyryl)-4H-pyran. [e] Sodium dodecyl sulfate. [f] Cetyltrimethylammonium bromide. [g] γ-Cyclodextrin. [h] Aerosol OT (0.09 M AOT in *n*-heptane). [i] Dimyristoylphosphatidylcholine.

* To whom correspondence should be addressed. FAX: +81-75-753-3975. E-mail: hara@kuchem.kyoto-u.ac.jp.

10.1021/jp0109776 CCC: $20.00
Published on Web 07/07/2001

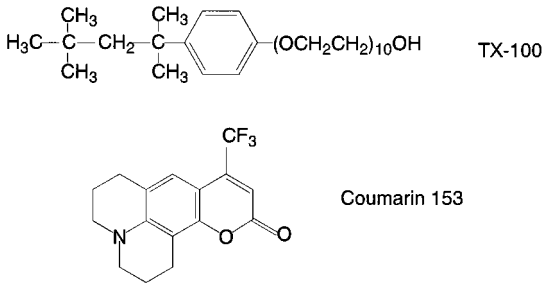

Figure 1. Structures of TX-100 and coumarin 153.

dependence of critical micelle concentration (cmc) has been determined previously.[19] Moreover, the C153 probe has been widely utilized as a representative of large polyatomic solutes whose excitation causes a large increase in dipole moment without serious change in specific solute−solvent interactions.

2. Experimental Section

Coumarin 153 (C153) (laser dye, Lambda Physik) and Triton X-100 (TX-100) (spectroscopic grade, Nacarai Tesque) were used as received. The concentration of TX-100 is 3.0×10^{-3} M. This is approximately 20 times higher than cmc ($\sim 2.6 \times 10^{-4}$ M), in which the change of cmc with pressure has no effect to form stable micelles. The probe concentration is 1.0×10^{-5} M, which is much lower than the micelle concentration, thereby minimizing the possible perturbation of the probe environment. When the aggregation number of TX-100 micelles is supposed as 120,[20] the average number of probe per micelle is calculated to be 0.4.

The high-pressure cell equipped with four sapphire windows and the pressure generating system used for the present measurements have been described previously.[21] Sample solution was provided in a quartz inner cell. All the steady-state and time-resolved fluorescence measurements at high pressures were performed at room temperature (~20 °C). The excitation wavelengths for steady-state and time-resolved measurements are 404.5 and 397.5 nm, respectively, where there is no absorption in TX-100. Fluorescence spectra were converted from a linear wavelength to linear frequency representation prior to analysis.

Time-resolved emission data at high pressures were collected on a laser system with a time-resolution of ca. 30 ps by using time-correlated single photon counting (TCSPC) technique. The TCSPC laser system and the method of data analysis have been described elsewhere.[22] The excitation light source is a Ti: sapphire laser (Spectra-Physics, Tsunami model 3950) with 82 MHz repetition rate. The pulse repetition rate was decreased to 26.8 MHz by using an electrooptic light modulator (Con Optic, model 1305). The instrument response function (IRF), that is determined by using the scattering of the solution at the excitation wavelength in the high-pressure cell, has a full width half-maximum (fwhm) of 30 ps, giving a time resolution better than 20 ps after signal deconvolution.

3. Results

A. Steady-State Spectra. In pure aqueous solution the solubility of C153 is too low to observe the emission spectrum. The low solubility of C153 in water is a primary reason we chose it as a probe, whereas in aqueous solution of TX-100 surfactant above cmc the probe is soluble enough to measure the emission spectrum with appreciable intensity, suggesting that the probe is predominantly incorporated into micelles. Such a discontinuous increase in fluorescence intensity at cmc has been employed as a reliable method of cmc detection for neutral surfactant at high pressures.[19]

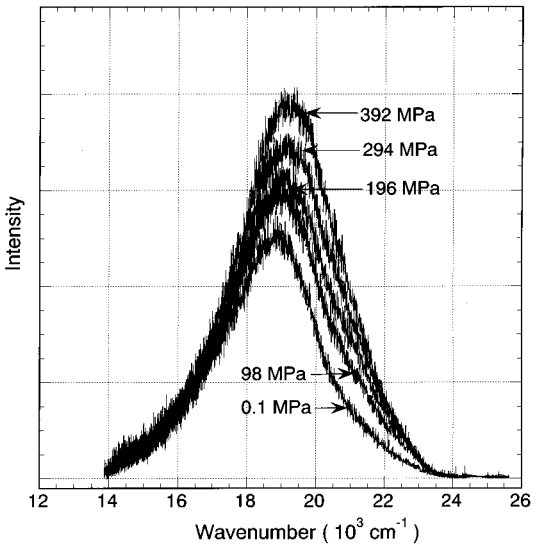

Figure 2. Steady-state fluorescence spectra of C153 in aqueous TX-100 surfactant micellar solution at different pressures.

In aqueous solution of TX-100 surfactant micelles the emission peak maximum ($\bar{\nu}_m$) of C153 at atmospheric pressure (0.1 MPa) is located at 18880 cm^{-1}. Examining the $\bar{\nu}_m$ values in pure solvents, we observe 18310 cm^{-1} for methanol, 18340 cm^{-1} for ethanol and 18600 cm^{-1} for 1-propanol[23]. Namely, $\bar{\nu}_m$ slightly increases with increasing the chain length of *n*-alcohols. Furthermore, for the case of nonpolar solvent, e.g., cyclohexane, it amounts 22030−23020 cm^{-1}. Here we find that the location of the emission maximum of C153 in the aqueous solution of TX-100 micelles is approximately equal to that in alcohol solvent. This suggests that the C153 probe feels a microenvironment having a polarity corresponding to alcohols, which is much more polar than hydrocarbon medium and less polar than pure bulk water medium. Therefore, we can conclude that the C153 probe molecule is not situated in the hydrocarbon-core region of the micelles, but in the intermediate solvated region, referred to as "Stern layer" of micelles. Similar result has also been reported previously by Bhattacharyya and co-workers.[6]

Figure 2 shows the fluorescence spectra of C153 in TX 100 micelles at different pressures. We see that the band intensity appreciably increases with pressure. By fitting them to the Gaussian type functional form around the peak, the peak maximum ($\bar{\nu}_m$) was determined as a function of pressure. As shown in Figure 3, pressure causes a linear blue shift having a rate of $d\bar{\nu}_m/dP = 1.34$ cm^{-1}/MPa. Conversely, in the case of ethanol solution it shifts toward red,[22] whose aspect is also included in Figure 3 for comparison. The extent of the pressure red shift $d\bar{\nu}_m/dP = -0.75$ cm^{-1}/MPa, which is somewhat larger than the case of typical $\pi-\pi^*$ transition for aromatic molecules,[24] reflects the charge-transfer character of C153 in the excited state, where a large increase in dipole moment is accompanied by the excitation.

It should be remembered that according to the study in a series of pure solvents at atmospheric pressure,[1] the fluorescence band of C153 shows blue shift with decreasing solvent polarity. In addition, it has been observed that the less polar is the medium the greater is the fluorescence intensity.[1] As the result, the pressure effects on the peak shift and the intensity of the fluorescence band leads to the conclusion that the increase in pressure produces a less polar environment. The possible

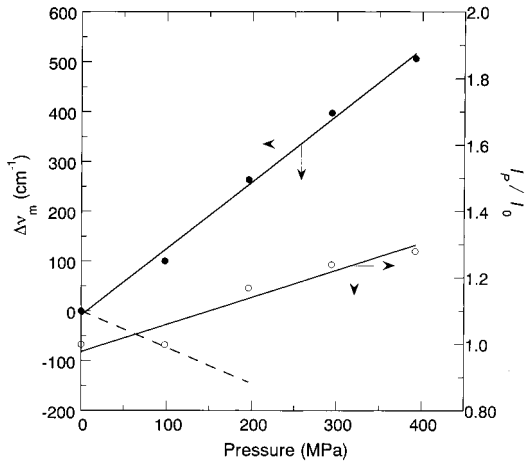

Figure 3. Pressure dependence on the intensity and peak maximum of C153 fluorescence band. The peak shift in ethanol solution is represented by the dased line for comparison.

reasoning for this behavior may be either the movement of the probe into the hydrocarbon-core region or the decrease of water penetration in the vicinity of the probe. Free water molecules may reside in the Stern layer and their diffusion will be substantially retarded with pressure.

B. Time-Resolved Spectra. In the aqueous micellar solution of TX 100 surfactant, the fluorescence decay of C153 is dependent on the wavelength detected. Figure 4 shows the typical fluorescence decay curves of C153 in the aqueous TX-100 surfactant solution above cmc at various wavelengths. The decays at the red end are significantly different from those at the blue end. The decays at the red end exhibit a distinct growth at every pressure. Such wavelength-dependent behavior of the fluorescence decay indicates that the fluorescence of C153 presents the time-dependent Stokes shift (TDFSS) in the micellar environment.

In case that the probe molecules reside in the hydrocarbon core of micelles, the TDFSS could not be observed. Conversely, if they are in bulk pure water phase, the solvation dynamics should be too fast to be observed in our present setup having a time resolution of ~20 ps. It should be noted that it has been observed that the solvation time of coumarin 480 in pure water falls at around 310 fs.[2] For this reason, the present appearance of the TDFSS provides a convincing evidence that the probe molecules locate in the Stern layer of the micelles, in which the TDFSS does reflect the solvation dynamics in the Stern layer.

Fluorescence decay data sets were collected at every 10 nm (13 different wavelengths) to span the entire steady-state spectrum at different pressures. The individual wavelength-dependent fluorescence decay curves were fitted to the sum of three exponentials using nonlinear least-squares regression algorithm. The instrument response function (IRF) was deconvoluted from the decay data. Figure 5 shows the representative reconstructed time-resolved fluorescence spectra of C153 in the aqueous solution of TX-100 surfactant above cmc at pressures of 0.1 and 392 MPa. The reconstructed spectral data points at time t were well fitted to a log-normal line shape function.[25] To obtain the best estimate of the time-dependent fluorescence, the peak frequency was employed. The time-dependent properties of the emission spectrum are generally quantified in terms of spectral response function ($C(t)$), which is defined by

$$C(t) = \frac{\tilde{\nu}(t) - \tilde{\nu}(\infty)}{\tilde{\nu}(0) - \tilde{\nu}(\infty)} \qquad (1)$$

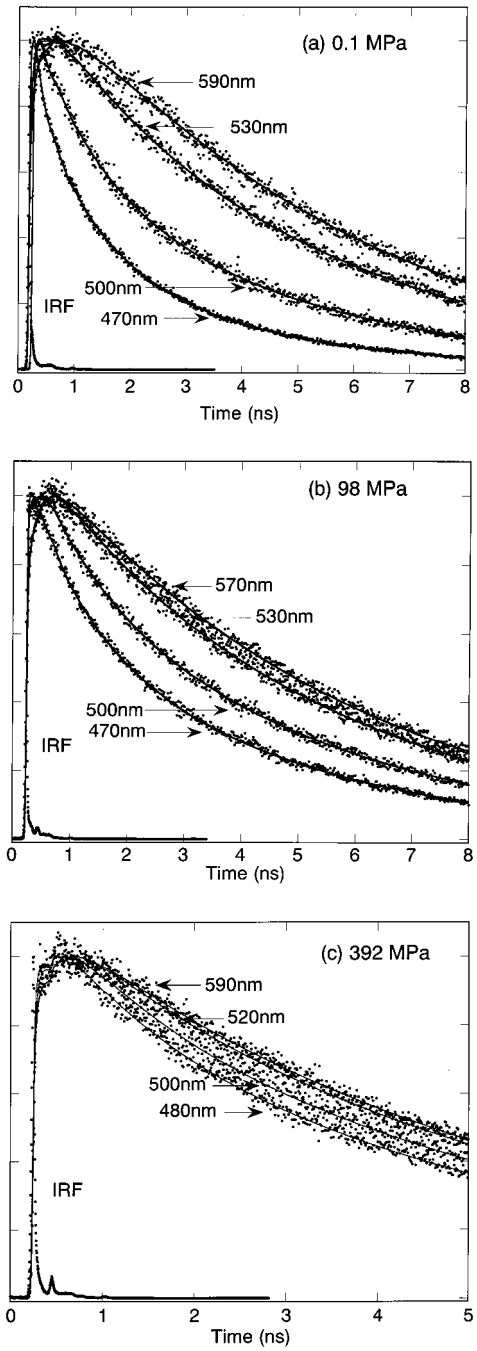

Figure 4. Representative fluorescence decays of C153 in TX-100 micelles at various wavelengths and at pressures of (a) 0.1 MPa, (b) 98 MPa, and (c) 392 MPa. They were plotted linearly and each intensity was normalized at the maximum. The solid line through the data points represent the best fit to a biexponential function.

where $\tilde{\nu}(t)$, $\tilde{\nu}(0)$, and $\tilde{\nu}(\infty)$ denote the fluorescence maxima observed at times t, zero, and infinity, respectively. It is this response function, which has been used as directly comparable to the theoretical prediction of solvation dynamics, since experimentally determined $C(t)$ is related to the response function of solvation energy relaxation under proper conditions.[26,27] The formation of the excited state of a probe molecule occurs more rapidly than nuclear rearrangement of solvent molecules, so that the excited-state probe finds itself initially (at $t = 0$) in a solvent configuration characteristic of the ground state. With increasing time, the solvent restructures in response to the charge distribution of the excited-state probe molecules. Namely, $C(t)$ provides a measure of the solvation relaxation

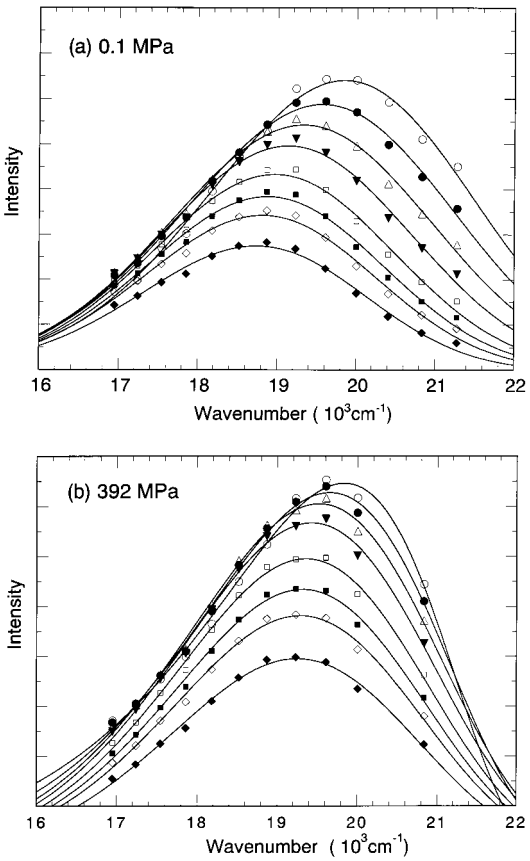

Figure 5. Time-resolved fluorescence spectra of C153 in TX-100 micelles at pressures of (a) 0.1 MPa and (b) at 392 MPa. Times after excitation are 0 ps (○), 100 ps (●), 250 ps (△), 500 ps (▼), 1000 ps (□), 1500 ps (■), 2000 ps (◊), and 3000 ps (♦). The solid lines through the data points represent the log-normal fits.

process. The spectral reconstruction method leading to the response function $C(t)$ has been described in detail by Maroncelli and Fleming.[28] The experimental $\tilde{\nu}(t)$ vs t data sets were well reproduced by

$$\tilde{\nu}(t) = \tilde{\nu}(\infty) + \Delta\tilde{\nu}\sum_{i}^{2} a_i \exp(-t/\tau_i) \qquad (2)$$

where $a_1 + a_2 = 1$. The value of $\tilde{\nu}(\infty)$ was determined as the wavenumber obtained from the asymptotic baseline of the biexponentially fitted curve. It should be noted that when the time scale of electronic deactivation is comparable to that of the solvation relaxation, which is the present case, the correct value of $\tilde{\nu}(\infty)$ cannot be obtained from the steady-state spectrum.

Figure 6 shows the typical reconstructed solvent response functions, $C(t)$ at pressures of 0.1, 196, and 392 MPa, which are well fitted to biexponential functions. The characteristic times thus obtained are listed in Table 2. At first, we see that the solvation in micelles clearly exhibits bimodal character, having the fast component (τ_1) 198 ps and the slow one (τ_2) 1.63 ns. The solvation times of the aqueous solution of TX 100 micelles has been observed so far by using different probes.[6,11,12] As seen in Table 1, in every case the time scale of the fast component falls 200−300 ps, and the slow one around 1−2 ns. Taking the difference in probe molecule as well as the experimental error bar into consideration, we can conclude that the agreement with previous results is satisfactory. It should be remembered that the time scale of the fast component is by about 3 orders of magnitude slower than the solvation time of

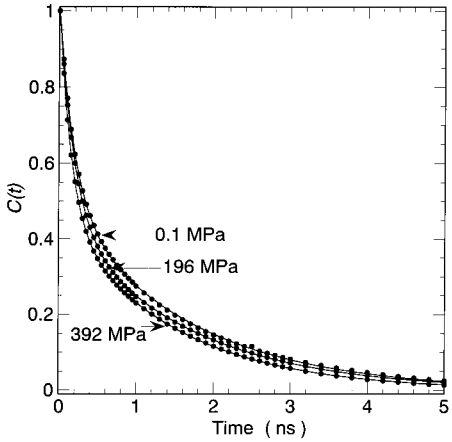

Figure 6. Decays of solvent response funtions, $C(t)$, reconstructed for C153 in TX-100 micelles at different pressures. The solid line represents the best fit to a biexponential decay.

TABLE 2: Spectral Shift ($\Delta\tilde{\nu}$), Solvation Times (τ_1, τ_2), Average Solvation Time ($\langle\tau\rangle$), and Amplitudes (a_1, a_2) of C153 in the Stern Layer of TX-100 Micelles at High Pressures

pressure (MPa)	$\Delta\tilde{\nu}$ (cm^{-1})	a_1	τ_1 (ps)	a_2	τ_2 (ps)	$\langle\tau\rangle$ (ps)
0.1	1210	0.50	198	0.50	1630	920
98	999	0.50	207	0.50	1720	967
196	781	0.54	198	0.46	1620	844
294	702	0.49	166	0.51	1400	792
392	619	0.54	158	0.46	1450	749

pure water.[2] Secondly, we find in the table that both time constants, τ_1 and τ_2, synchronously change with pressure. Namely, they increase at 98 MPa and decrease at higher pressures. Also included in Table 2 is the average solvation time $\langle\tau\rangle$, which is defined by $\langle\tau\rangle = a_1\tau_1 + a_2\tau_2$. In most cases, the solvation dynamics has been discussed by means of the $\langle\tau\rangle$ value.

Another important consideration in time-resolved studies of solvation is to determine the total spectral shift resolved by experiment. The observed total dynamic spectral shifts, $\Delta\tilde{\nu} = \tilde{\nu}(0) - \tilde{\nu}(\infty)$, are also included in Table 1. It is usual that the experimentally resolved time-zero spectrum is far to the red of the real time-zero spectrum. Fee and Maroncelli[29] have developed a procedure for estimating the time-zero spectrum in time-resolved experiments. The estimated total dynamic shift for C153 is ∼4500 cm^{-1}. It follows that more than half of the total Stokes shift is estimated to occur more quickly than observed in our TCSPC experiments.

Further, we can see in the table that the $\Delta\tilde{\nu}$ value decreases with increasing pressure. This is considered as due to the fact that with increasing pressure the amount of water molecules which may affect the solvation decreases to produce a less polar environment. Here, it should be noted that the deactivation time of the S_1-state did not exhibit any appreciable change with pressure, which is observed by the decay time longer than 10 ns. This finding is just correlated to the conclusion in the steady-state experiment that the pressure provides a less polar environment. As a consequence, the pressure effect on the solvation dynamics can be explained by the schematical illustration in Figure 7, indicating how the blue shift of the spectrum with pressure is related to the decrease in $\Delta\tilde{\nu}$.

4. Discussions

From the present steady-state and time-resolved fluorescence studies, we can conclude that the C153 probe molecule in the

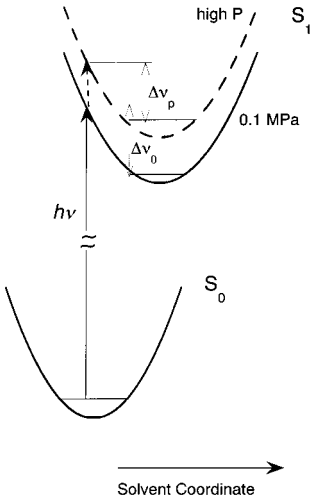

Figure 7. Illustration indicating the pressure dependence on the TDFSS process related to the solvation dynamics in TX-100 micelles. $\Delta\upsilon_0$ and $\Delta\upsilon_p$ represent the shift at atmospheric pressure and at high pressure, respectively.

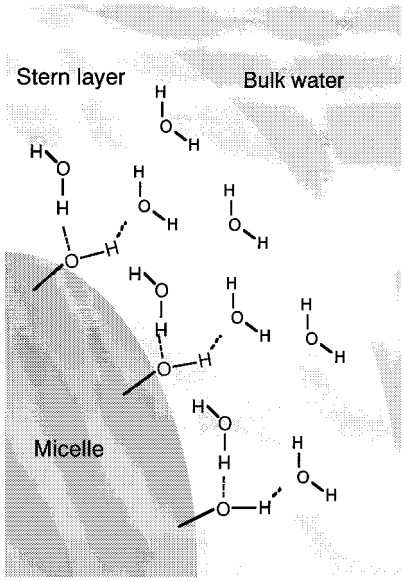

Figure 8. Schematic illustration of the Stern layer of micelles.

aqueous solution of TX-100 surfactant micelle feels a microenvironment which is quite different from the bulk water as well as from the hydrocarbon-core region of the micelle. Namely, the probe molecule should be located in the intermediate solvated region, named as the "Stern layer" of micelles, where the polarity is higher than that in hydrocarbon medium and lower than that in pure bulk water medium. Figure 8 illustrates the schematic view of the Stern layer structure surrounding a micelle, reported as having a thickness around 2.5 nm for neutral micelle.[30] It is consisted from many layers of water molecules. Between the Stern layer and bulk water there is a diffuse and loose layer called the "Guoy−Chapman layer", although not drawn in the figure, where water molecules are expected to move much faster than in the Stern layer.[31] A water molecule just in the vicinity of a micelle should be engaged in two types of hydrogen bond, i.e., one is the bond with other water molecules, and the other is with the headgroup of the micelle. If the probe presented in the bulk water, then the solvation dynamics should be observed in subpicosecond time scale, which cannot be detected with our current experimental time resolution. The solvation response of C153 dissolved in pure water has been considered very fast, which is completed within 1 ps.[1] Conversely, if it were in the hydrocarbon-core region, then the time-dependent Stokes shift could not be observed.

From the result of the pressure dependence on the steady-state fluorescence spectrum, we found that the increase of pressure produces a less polar environment. Possible causes explaining this pressure effect are (1) the suppression of the water penetration into the Stern layer (or the squeeze the water molecules residing in the Stern layer in the vicinity of the C153 molecule) and (2) the movement of the probe toward the less polar hydrocarbon-core region. When the finding of the decrease $\Delta\tilde{\nu}$ in is taken into account, the former will be the case.

From the TDFSS analysis, on the other hand, we found that the solvation dynamics of C153 exhibited distinct bimodal character. The possible origins causing the bimodal solvation dynamics will be closely related to the motion of the polar headgroup of the micelle and the motion of restricted water molecules in the micellar Stern layer. If the former is a large amplitude motion associated with methylene chain, it will be ruled out, since the motion of the polar headgroups of the surfactant is considered as quite restricted and the chain dynamics should occur in much longer time scale ($\sim$100 ns[32]) as compared with the present time scale. Nevertheless, a small amplitude headgroup motion just in the vicinity of the probe will be possible. And the other possibility will be the solvation time arising from the reorientation of highly constrained hydrogen-bonded water molecules.

As seen in Table 1, such bimodal solvation dynamics has previously been observed on the bases of the TDFSS studies in various aggregated molecular systems other than micelles, such as the water pool of reverse micelles,[7,8] water molecules included in cyclodextrins,[2] or in the aqueous solution of vesicles.[10,13] The longer solvation times in reverse micelle and vesicle as compared with micelle or cyclodextrin are considered as representing the more restricted state of water molecules. Namely, the more constrained the water molecules are, the slower should be the solvation time. In addition, the solvation time is dependent on the probe molecule. The coumarin shows a longer solvation time. This will be associated with its smaller solubility in water. The probe 4-aminophthalimide (4AP) which is the more soluble in water possesses a faster solvation time, whose aspect is seemingly the more sensitive to the longer component.

According to the model proposed by Nandi and Bagchi,[33] which has originally been described for the dielectric relaxation due to water molecules in the hydration shell of biological molecules such as proteins, the bimodal relaxation arises from a dynamic equilibrium between "bound water" and "free water" in the hydration shell of biomolecules, described by two widely different characteristic time constants; one of which is in the picosecond while the other is in the nanosecond time scale. According to this model, it has been proved that the relaxation component is related to the strength of the hydrogen bond with the headgroups of biomolecules in the hydration shell. Furthermore, it has been expected that it should become faster with decreasing the strength of the hydrogen bond. The observed bimodal solvation behavior and its pressure dependence on the dynamic Stokes shift of the C153 probe in aqueous TX-100 micellar solution can be well explained within the framework of the similar model proposed by Nandi and Bagchi.[33]

When we suppose an analogous equilibrium between the restricted "bound water" and "free water" in the micellar Stern layer, the instantaneous dipole change in the probe upon electronic excitation does disturb the equilibrium and relaxes

to a new equilibrium in the vicinity of the probe. This may also cause the bimodal relaxation in the solvation dynamics. And it may follow that the relaxation time becomes faster as the pressure increases, since the strength of hydrogen bonding is weakened with increasing the pressure. It has been known that, on the basis of high-pressure studies of the rotational correlation time (τ_{2R}) for water molecules, the application of high pressure causes a distortion of hydrogen bond and weakens its strength.[34]

The anomalous increase in solvation time at lower pressure less than 98 MPa is reproducible and seems beyond the error bar of the present experiment. This may be caused by the initial larger restriction of the water motion in the Stern layer, but when we bear the complicated behavior of water in mind, the more detailed research would be required before concluding finally.

Acknowledgment. This work was supported in part by the Grant-in-Aid for Scientific Research (No. 09640602) from the Ministry of Education, Science, Sports and Culture. Additional support was provided by Core Research for Evolutional Science and Technology (CREST) of Japan Science and Technology Corporation (JST). We thank Prof. Kankan Bhattacharyya for helpful discussions.

References and Notes

(1) For example, Horng, M. L.; Gardecki, J. A.; Papazyan, A.; Maroncelli, M. *J. Phys. Chem.* **1995**, *99*, 17311 and references therein.
(2) Vajda, S.; Jimenez, R.; Rosenthal, S. J.; Fidler, V.; Fleming, G. R.; Castner, E. W., Jr. *J. Chem. Soc., Faraday Trans.* **1995**, *91*, 867.
(3) Jimenez, R.; Fleming, G. R.; Kumar, P. V.; Maroncelli, M. *Nature* **1994**, *369*, 471.
(4) Menzel, K.; Rupprecht, A.; Kaatze, U. *J. Phys. Chem. B* **1997**, *101*, 1255.
(5) Urry, D. W.; Peng, S.; Xu, J.; McPherson, D. T. *J. Am. Chem. Soc.* **1997**, *119*, 1161.
(6) Sarkar, N.; Datta, A.; Das, S.; Bhattacharyya, K. *J. Phys. Chem.* **1996**, *100*, 15483.
(7) Sarkar, N.; Das, K.; Datta, A.; Das, S.; Bhattacharyya, K. *J. Phys. Chem.* **1996**, *100*, 10523.
(8) Das, S.; Datta, A.; Bhattacharyya, K. *J. Phys. Chem. A* **1997**, *101*, 3299.
(9) Weiss, G. R.; Ramamuthy, V.; Hammond, G. S. *Acc. Chem. Res.* **1993**, *26*, 530.
(10) Datta, A.; Pal, S. K.; Mandal, D.; Bhattacharyya, K. *J. Phys. Chem. B* **1998**, *102*, 6114.
(11) Datta, A.; Mandal, D.; Pal, S. K.; Das, P.; Bhattacharyya, K. *J. Mol. Liq.* **1998**, *77*, 121.
(12) Pal, S. K.; Sukul, D.; Mandal, D.; Sen, S.; Bhattacharyya, K. *Chem. Phys. Lett.* **2000**, *327*, 91.
(13) Pal, S. K.; Sarkar, D.; Mandal, M.; Bhattacharyya, K. *J. Phys. Chem., B* **2000**, *104*, 4529.
(14) Nandi, N.; Bhattacharyya, K.; Bagchi, B. *Chem. Rev.* **2000**, *100*, 2013.
(15) Nandi, N.; Bagchi, B. *J. Phys. Chem.* **1996**, *100*, 13914.
(16) Hara, K.; Ito, N. *Recent Dev. Phys. Chem.* **1998**, *2*, 947. Hara, K. *Trends Chem. Phys.* **1997**, *5*, 57.
(17) Kometani, N.; Kajimoto, O.; Hara, K. *J. Phys. Chem. A* **1997**, *101*, 4916.
(18) Polyehtylene glycol mono-*p*-isooctylphenyl ether with a molecular weigh of 95 000.
(19) Hara, K.; Kuwabara, H.; Kajimoto, O.; Bhattacharyya, K. *J. Photochem. Photobiol.* **1999**, *124*, 159.
(20) Tummino, P. J.; Gafni, A. *Biophys. J.* **1993**, *64*, 1580.
(21) Hara, K.; Morishima, I. *Rev. Sci. Instrum.* **1988**, *59*, 2397.
(22) Hara, K.; Kometani, N.; Kajimoto, O. *Chem. Phys. Lett.* **1994**, *225*, 381.
(23) Baden, N.; Hara, K. Unpublished data.
(24) For example, Offen, H. W. In *Organic Molecular Photophysics*; Birks, J. B., Ed.; John Wiley & Sons: 1973; Vol. 1, p 103. Hara, K.; W. Rettig, *J. Phys. Chem.* **1992**, *96*, 8307.
(25) Fraser, R. D. B.; Suzuki, E. In *Spectral Analysis*; Blackburn, J. A., Ed.; Marcel Dekker: New York, 1970; p 171.
(26) Bagchi, B.; Oxtoby, W.; Fleming, G. R. *Chem. Phys.* **1984**, *86*, 257.
(27) van der Zwan; Hynes, J. T. *J. Phys. Chem.* **1985**, *89*, 4181.
(28) Maroncelli, M.; Fleming, G. R. *J. Chem. Phys.* **1988**, *88*, 5044.
(29) Fee, R. S.; Maroncelli, M. *Chem. Phys.* **1977**, *99*, 8127.
(30) Paradies, H. H. *J. Phys. Chem.* **1980**, *84*, 599.
(31) Saroja, G.; Samanta, A. *Chem. Phys. Lett.* **1995**, *246*, 506.
(32) Datta, R.; Chowdburry, M.; Winnik, M. A. *Polymer* **1995**, *36*, 4445.
(33) Nandi, N.; Bagchi, B. *J. Phys. B* **1997**, *101*, 10954.
(34) (a) Wakai, C.; Nakahara, M. *J. Chem. Phys.* **1994**, *100*, 8347. (b) Nakahara, M.; Wakai, C. *J. Mol. Liq.* **1995**, *65/66*, 149.